Plasticity of human auditory-evoked fields induced by shock conditioning and contingency reversal

Christian Kluge[a,b,c,1], Markus Bauer[a], Alexander Paul Leff[b], Hans-Jochen Heinze[c], Raymond J. Dolan[a], and Jon Driver[a,b]

[a]Wellcome Trust Centre for Neuroimaging, University College London, London WC1N 3BG, United Kingdom; [b]Institute of Cognitive Neuroscience, University College London, London WC1N 3AR, United Kingdom; and [c]Department of Neurology, Otto von Guericke University, D-39120 Magdeburg, Germany

We used magnetoencephalography (MEG) to assess plasticity of human auditory cortex induced by classical conditioning and contingency reversal. Participants listened to random sequences of high or low tones. A first baseline phase presented these without further associations. In phase 2, one of the frequencies (CS+) was paired with shock on half its occurrences, whereas the other frequency (CS−) was not. In phase 3, the contingency assigning CS+ and CS− was reversed. Conditioned pupil dilation was observed in phase 2 but extinguished in phase 3. MEG revealed that, during phase-2 initial conditioning, the P1m, N1m, and P2m auditory components, measured from sensors over auditory temporal cortex, came to distinguish between CS+ and CS−. After contingency reversal in phase 3, the later P2m component rapidly reversed its selectivity (unlike the pupil response) but the earlier P1m did not, whereas N1m showed some new learning but not reversal. These results confirm plasticity of human auditory responses due to classical conditioning, but go further in revealing distinct constraints on different levels of the auditory hierarchy. The later P2m component can reverse affiliation immediately in accord with an updated expectancy after contingency reversal, whereas the earlier auditory components cannot. These findings indicate distinct cognitive and emotional influences on auditory processing.

Seminal animal studies revealed experience-dependent plastic changes in auditory cortex (e.g., refs. 1–3; reviewed in refs. 4–6). Such plasticity can emerge rapidly, persist, and relate to neuromodulation. Auditory plasticity can reflect stimulus features as well as top-down, task-related factors (e.g., ref. 7).

Most research on auditory plasticity involved rodents, cats, or nonhuman primates, but some related evidence comes from human neuroimaging studies, with PET (8, 9) or functional (f) MRI (10). Here, we used magnetoencephalography (MEG) (11, 12) to address human auditory plasticity in an aversive classical-conditioning paradigm (1–3), focusing on the well-known, successive, auditory-evoked field components P1m, N1m, and P2m (13, 14). Other human EEG or MEG work on conditioning typically used a visual rather than auditory CS+ (15–17, but see ref. 11).

MEG enabled us to study conditioning effects upon auditory responses with temporal precision and whether such effects can reverse when contingencies change (e.g., when the former CS+ now becomes the CS− and vice versa). This approach allowed us to distinguish modulation of auditory sensory responses that can flexibly reverse with a sudden change in contingency (consistent with top-down cognitive mediation, as turned out to be the case for the P2m) versus modulation that is not readily reversed (as it turned out for the P1m). We assessed this by examining auditory-evoked fields during three successive phases of our MEG experiment. Phase 1 was before introduction of any shock association; phase 2 shocked half the CS+ presentations but never CS−, whereas for final phase 3, assignment of CS+/CS− was abruptly reversed relative to phase 2, with our human participants being informed of this new contingency. Although our main focus was on auditory MEG responses, for completeness we concurrently measured any conditioning impacts upon pupil dilation (18–22).

Results

Pupil Responses. Shock application should lead (18–22) to pupil dilation as an unconditioned response (UR). We further measured whether classical conditioning of specific tone-shock pairings led to conditioned pupil dilation (18–22) to CS+ as a conditioned response (CR). Fig. 1A shows a UR manifest as increased pupil dilation, peaking ~2 s after shock onset. This UR was equivalent for phases 2 and 3, indicating it did not habituate. None of the time points show significant differences between phases 2 and 3 on paired t test, all P > 0.2, NS.

We also analyzed pupil responses for CS− and for those CS+ trials without shock (to avoid cross-contamination by the UR). Fig. 1B shows pupil dilation time locked to tone onset, shown separately for current CS+ versus CS−. This analysis revealed a conditioned response for phase 2 in the form of enhanced pupil dilation for CS+, peaking ~2.75 s after tone onset. The difference between CS+ and CS− was significant (P < 0.05 by paired t test) throughout the time window indicated in Fig. 1B for phase 2 data. However, no conditioned pupil response was apparent in the phase 3 data (Fig. 1C). Thus, the pupil CR did not undergo reversal, in terms of tone affiliation, after contingency reversal, but rather "extinguished" then (23–26). This remains the case even when considering only later parts of phase 3. For instance, in just the final quarter of trials within phase 3, there remained no pupil dilation difference between the new CS+ versus the new CS− (P = 0.78, NS).

When turning to the MEG data below, we find analogously to the pupil data that some early auditory-evoked fields (P1m) showed a conditioning effect (i.e., significant CS+/CS− difference) within phase 2 that did not reverse to an opposite effect within phase 3, but rather was eliminated then. By contrast, the later auditory-evoked field (notably P2m) was able to show rapid reversal after the contingency change.

Auditory-Evoked Fields in MEG. *Selection of time windows and sensors of interest for auditory-evoked fields.* MEG data were time locked to tone onset to compare auditory-evoked fields for CS+ versus CS− for phases 2 and 3. The actual tone frequency serving as CS+ was counterbalanced across participants. In order to define sensors and time windows of interest in an unbiased way, we first considered auditory-evoked fields from the "baseline" blocks of phase 1, regardless of tone frequency, prior to any shock conditioning.

Fig. 2A shows butterfly plots of all sensors, plus field topographies for the three successive time windows indicated, from phase 1. The three time windows indicated were selected on the basis of the butterfly plots shown to encompass the well-known P1m auditory-evoked field within a 35–65 ms time window post tone onset, the well-known N1m auditory-evoked field within 85–115 ms, and the P2m component within 180–270 ms.
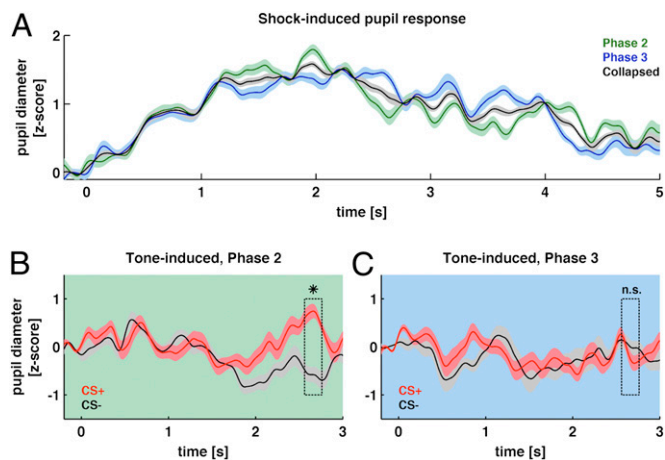
Fig. 1. (*A*) Grand mean pupil diameter (as *z* scores) plotted against time since shock-US onset, shown for initial conditioning phase 2 (in green), for contingency reversal phase 3 (in blue), and also pooled across these two phases (shown in black). For both phases 2 and 3, the shock-US consistently induced pupil dilation as an unconditioned response (UR), which peaked ~2 s after shock-US onset. Thus, the pupil UR did not habituate away in phase 3 versus phase 2, i.e., the shock-US remained potent. (*B*) Grand mean pupil diameters (again as *z* scores), now plotted against time since onset of the tone (CS⁺ or CS⁻), for phase 2. Note that CS⁺ induces significantly larger pupil dilation (now as a conditioned response, CR) than CS⁻ in phase 2, peaking around ~2.6 s after sound onset. (*C*) Pupil diameter did not show a consistent conditioned response to the (reassigned) CS⁺ versus CS⁻ in phase 3 following contingency reversal; rather the pupil CR became "extinguished" (main text).

To select sensors of interest (27) for auditory-evoked fields in these time windows, the planar gradient (Fig. 2*B*) of the field topography for each of the three components was calculated. Three sensors over temporal cortex displaying maximal amplitudes in response to tones within phase 1 (i.e., prior to any conditioning) were selected in each hemisphere (Fig. 2). Inspection of the topographies in Fig. 2 *A* and *B* provides visual confirmation that the selected sensors corresponded well with a clear dipolar pattern. Because this prior selection of time windows and sensors of interest was based solely on the pre-conditioning data from

phase 1, it was unbiased with respect to subsequent comparisons of CS⁺ and CS⁻ for phase 2 (initial conditioning) and phase 3 (contingency reversal), thereby avoiding circularity (28).

Phase 2 effects of initial conditioning on auditory-evoked fields for CS⁺ versus CS⁻. Pairing one tone but not the other with shock in phase 2 led to significant differences in the amplitude of the planar gradient auditory-evoked fields for CS⁺ versus CS⁻ (Fig. 3). Fig. 3*A* shows data for the P1m component, Fig. 3*B* for the N1m, and Fig. 3*C* for the P2m. The bar plots depict the mean data across all of phase 2 (with phase-1 baselines shown also, by the dashed bars), whereas the line graphs at *Right* reveal how the CS⁺ versus CS⁻ differences evolve over the course of phase 2, for six successive trial bins (successive sixths of the total trials run in that phase).

Note that for the P1m field (Fig. 3*A*, *Left* bar plot), the amplitude was actually *reduced* (Discussion) for CS⁺ relative to CS⁻ ($t(14) = 2.93$; $P = 0.01$). By contrast, for N1m (Fig. 3*B*) and P2m (Fig. 3*C*) fields, the amplitude was significantly *increased* for CS⁺ relative to CS⁻ ($t(15) = 2.29$; $P = 0.0367$ for N1m and $t(15) = 4.74$; $P = 0.0005$ for P2m, respectively). However, for all three components, the critical point is that significant differences in amplitude emerged for CS⁺ versus CS⁻ due to the shock association introduced in phase 2. Note that we analyzed only *unshocked* CS⁺ trials for N1m and P2m to avoid contamination of evoked fields by the shock event, whereas for P1m, we analyzed all trials because its time window preceded the shock.

When considering how these effects arise for the six successive parts of phase 2 (Fig. 3, *Right* line graphs), it is evident that for all three auditory components, the conditioning effect emerges rapidly, within the first bin of phase 2 (i.e., within just 30 trials of the shock being introduced). A two-way ANOVA for each evoked field component (i.e., P1m, N1m, or P2m), with factors of conditioning (CS⁺ versus CS⁻) and successive trial bins (1–6) of phase 2, revealed a main effect of conditioning for P1m ($F(1,168) = 7.33$; $P < 0.008$), for N1m ($F(1,180) = 14.15$; $P < 10^{-4}$), and for P2m ($F(1,180) = 51.42$; $P < 10^{-12}$), but no main effect or interaction involving trial bin (1–6) within phase 2 for any component (all $P > 0.4$, NS). The apparent trend for some reduction in the CS⁺/CS⁻ difference for P1m toward the end of phase 2 did not approach significance.

These phase 2 results demonstrate that the shock contingency affects the amplitude of auditory-evoked fields in MEG. The MEG components came to distinguish CS⁺ from CS⁻, thereby indicating plasticity in the auditory sensory response. Here, this
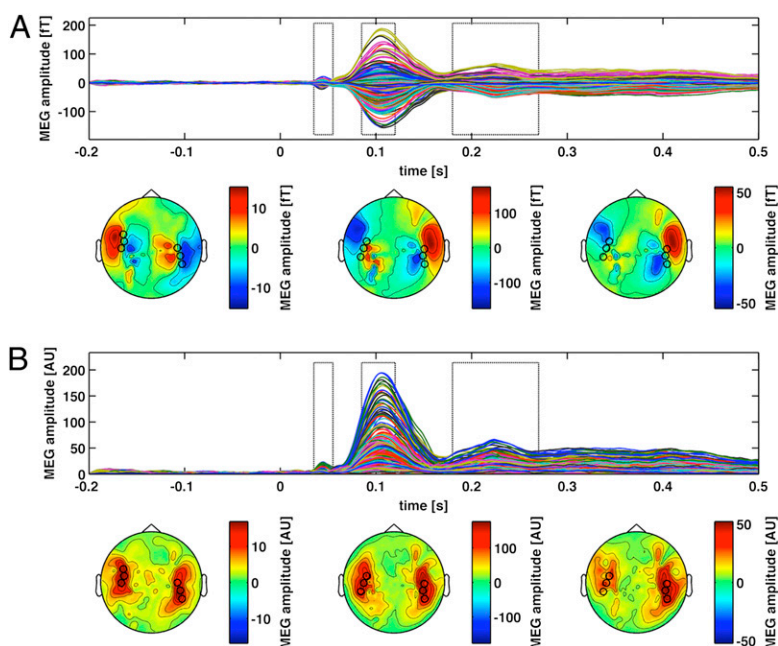

Fig. 2. (*A*, *Upper*) Butterfly plot for all MEG channels, time locked (at 0 along the *x* axis) to tone onset, collapsing across auditory frequency, in the preconditioning trials of phase 1 (i.e., before any shock was introduced), across participants. Note the clear response to the tone in the three time windows indicated (30–50, 85–115, and 180–270 ms). Mean topographies are shown below for these three time windows (now successively ordered left to right). (*B*) Data now replotted as planar gradients, with same time windows indicated. The black circles on the topographies indicate the sensors of interest selected from these preconditioning auditory responses, for each of the three time windows, as described in the main text. For completeness, these same selected sensors are also shown for the topographies in *A*. Note that the three components of interest (P1m, N1m, and P2m; see main text) each exhibit clear dipolar patterns (*A*), with maxima over temporal sites as confirmed in *B*, all as expected, given many previous auditory MEG studies on these components.
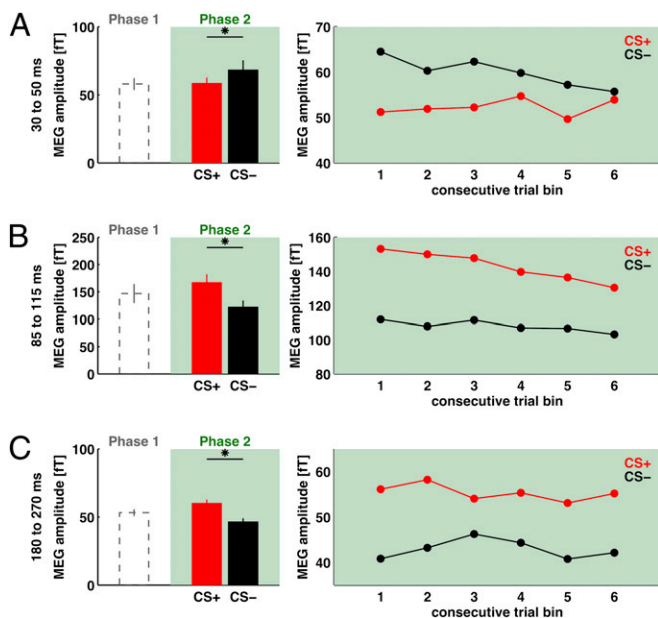
Fig. 3. (*A*) Bar plot (*Left*) shows intersubject mean P1m amplitude across the sensors of interest, collapsed across both tones before any conditioning (to provide a phase-1 baseline; dashed bar at far left) as well as for CS+ (red) or CS− (black) in the initial conditioning phase 2. Note the significant difference between CS+ and CS− for phase 2, indicating a conditioning influence on this early auditory response. The line graph (*Right*) shows P1m amplitude for CS+ or CS− across six successive "bins" of trials within phase 2, confirming that the conditioning influence was present from the very first such bin. (*B*) Results for the N1m component, showing a significant conditioning influence overall for phase 2 in the bar plot (now taking the form of higher amplitude for CS+ than CS−). The line graph (*Right*) confirms that this conditioning effect on N1m was again present from the first bin of trials and was then sustained across the subsequent five further bins of trials in phase 2. (*C*) Results for the P2m component, showing a similar conditioning effect in phase 2 as for the N1m component.

plasticity was evident within 35–65 ms of tone onset (for P1m) and also for later evoked auditory fields (N1m and P2m). It developed rapidly, being evident in the first part of phase 2 (Fig. 3, line graphs). We next consider whether such conditioning effects on human auditory responses, which can evidently arise rapidly, can be reversed when the tone-shock contingency reverses abruptly.

Phase 3 effects of contingency reversal on auditory-evoked fields. Fig. 4 plots the data for phase 3 (solid colors in bar plot, solid functions in line graph, on blue background), which reversed the contingencies so the previously unshocked tone frequency was now paired with shock and the previously shocked tone was not, as participants were informed (*Materials and Methods*). The equivalent results from the preceding phase 2 are also replotted in Fig. 4 (dashed bars and lines toward *Left* of histograms and *Left* of line graphs, on green background) to allow direct visual comparison. Data are shown separately for each of the evoked fields considered (P1m in Fig. 4*A*, N1m in Fig. 4*B*, and P2m in Fig. 4*C*). The CS+ assignation (and coloring) in Fig. 4 now refers to the current CS+ in phase 3 (which had been the CS− in phase 2) and analogously for the current CS− of phase 3 in Fig. 4.

The striking observation is that the conditioned modulation of the later P2m auditory-evoked field (Fig. 4*C*) rapidly reversed to the new assignment when the contingency was switched, doing so fully even within the first part of phase 3 (Fig. 4*C*, *Right* line graph), hence within 30 shocks. By contrast, the conditioned modulation never reversed to the new assignment for N1m and P1m, being extinguished instead for these components, somewhat similarly to the pupil response (although N1m did show some initial new learning for CS+ within the first bin of phase 3, which showed a marked (and significant, see below) increase in

N1m amplitude compared with phase 2 (Fig. 4*B*, *Right* line graph). Thus, even though all three auditory-evoked fields (P1m, N1m, and P2m) had readily displayed initial conditioned modulation in phase 2 (Fig. 3, line graphs or Fig. 4, dashed lines), these auditory MEG components showed a markedly different sensitivity to contingency reversal in phase 3. P2m rapidly showed complete reversal in its affilation; N1m showed some rapid plasticity of response but not reversal; P1m showed only an extinction-like pattern (the apparent trend for some CS+/CS− differentiation for P1m toward the very end of phase 3 did not approach significance).

These various outcomes were confirmed in three-way repeated-measure ANOVAs on each component, with factors of "conditioning" (CS+/CS−), "phase" (2/3), and "trial bin" (1–6, as per the *x* axis of the line graphs in Fig. 4). For P1m, no significant terms for trial bin were revealed, but a significant interaction of conditioning and experimental phase ($F_{(1,341)} = 5.75$; $P = 0.017$), due to CS+/CS− differences in phase 2, but not phase 3 (Fig. 4*A*) for P1m. These effects were confirmed by separate two-way ANOVAs (conditioning × trial bin) for P1m in phase 2 or 3, that revealed just a main effect of conditioning for phase 2 ($F_{(1,168)} = 7.33$; $P < 0.008$) but none for phase 3 ($P > 0.9$, NS), consistent with an "extinction" pattern for P1m in the latter.

Similarly a three-way ANOVA on the N1m revealed a significant interaction between conditioning and phase ($F_{(1,365)} = 14.41$; $P = 0.0002$), but no significant term involving trial bins 1–6. When analyzing phase 2 or phase 3 alone, we found a signifi-
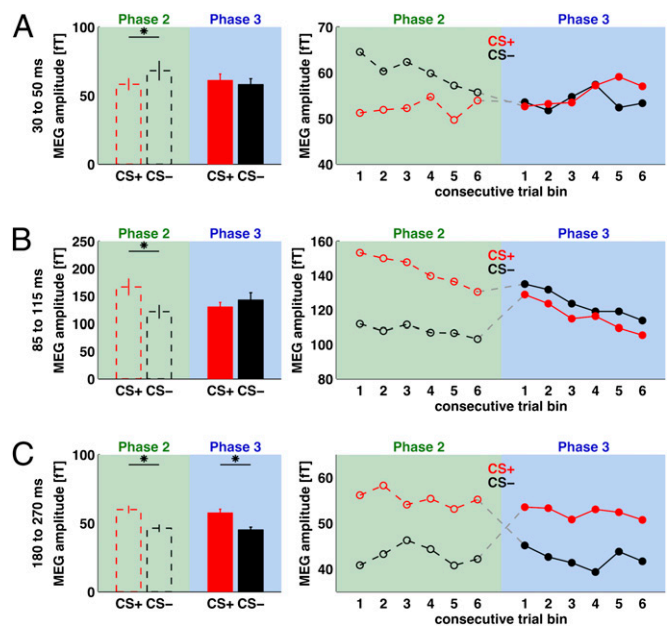

Fig. 4. The dashed lines within the bar plots and line graphs (shown on green backgrounds here) are data replotted from phase 2 (Fig. 3), shown again here to allow visual comparison with the new data subsequently acquired in phase 3 (shown here with filled bars, filled points and solid lines, against blue backgrounds) after the contingency reversal. Please note that CS+ and CS− (results shown in red or black) are coded here in terms of the current shock contingency. Thus, the particular tone frequency that served as CS+ during phase 2 actually became the CS− during phase 3, and vice versa. (*A*) Amplitude data for the P1m; (*B*) for the N1m; and (*C*) for the P2m. Note the different patterns of results for phase 2 versus phase 3. In phase 2, all three components (P1m, N1m, and P2m) came readily to distinguish CS+ and CS−, from the very first bin of trials. For phase 3, the P2m rapidly reversed its affiliation following the contingency change (*C*). The N1m showed some new learning but never reversed its affiliation (*B*). The P1m did not show significant reversal learning (the apparent trend for some crossover in bins 5 and 6 of phase 3 for P1m was far from reliable, $P > 0.7$). P1m showed no reliable CS+/CS− differentiation for phase 3, unlike phase 2.

cant effect of conditioning on the N1m in phase 2 ($F(1.180) = 18.15$; $P < 0.0001$), but not in phase 3 ($P > 0.4$). Although the new CS^+ did not differ from the new CS^- (former CS^+) within phase 3 overall for the N100, the line graph at *Right* of Fig. 4*B* nevertheless shows that N1m amplitude to the new CS^+ (former CS^-) appears to increase at the very start of phase 3, indicating some degree of rapid plasticity. A paired *t* test confirmed that in trial bin 1 of phase 3, the N1m evoked by the new CS^+ was larger than the response to the same stimulus when it had served as CS^- across all trial bins of phase 2 ($t(15) = 4.55$; $P < 0.0004$).

For the P2m component, three-way ANOVA showed a main effect of conditioning ($F(1,365) = 93.05$, $P < 10^{-12}$), but no other significant terms. This finding reflects the fact that the P2m showed a conditioning effect that was sustained across phase 2 but then immediately "reversed" its assignment (to follow the new CS^+/CS^-) when the contingency was reversed for phase 3, with this reversed effect then being sustained. To emphasize that this pattern does reflect flexibility, we also rescored the P2m data for phase 3 in terms of the original $CS^{+/-}$ assignment from phase 2. Viewed this way, the three-way ANOVA now yielded a highly significant interaction between (original) $CS^{+/-}$ and phase ($F(1,365) = 93.09$, $P < 10^{-12}$), due to the complete reversal in effect with contingency change for P2m.

Discussion

Using MEG, we observed plasticity for human auditory-evoked field components, with modulation of the auditory sensory response due to a classical contingency that paired shock with one heard frequency but not another. Importantly, these effects differed for distinct auditory components, in relation to the impact of an abrupt reversal in shock contingency. The earliest component, P1m beginning ~30 ms after sound onset, readily acquired differentiation between CS^+ and CS^- (within the first trial bin, therefore with just 30 shocks). Two later components, the N1m and P2m, were also readily influenced by the classical-contingency influence from the first trial bin of phase 2 onward, with these components showing higher amplitude for CS^+. However, when the shock contingency was suddenly reversed, this manipulation impacted on the three components in distinct ways, pointing to separable influences. The P2m rapidly reversed its affiliation, so that within the very first trial bin of phase 3 (with just 30 shocked trials for the new CS^+), it already showed higher amplitude for the new CS^+ that had previously been the CS^-. The N1m showed some rapid plasticity in response but never reversed its affiliation; instead, the CS^+/CS^- difference became absent. The earliest component, P1m, likewise did not significantly reverse its affiliation, with the CS^+/CS^- difference becoming absent/extinguished in phase 3, reminiscent of the outcome for pupil dilation. Observing such an extinction rather than a reversal for some components when the contingency changed here, might potentially reflect the large number of massed conditioning trials we used (e.g., 1,680 trials within phase 2, at 750- to 1,150-ms intervals). It is especially striking that, in phase 3, the pupillary response exhibited extinction to the previous CS^+ but failed to develop conditioning to the new CS^+. However, a key finding here was that, whereas the pupil, P1m, and N1m were unable to reverse their affiliations when the contingency reversed under these parameters, the P2m nevertheless fully reversed its affiliation, indicating more flexibility at this level of the auditory response.

The N1m and P2m showed higher amplitude for CS^+ than CS^-, in the initial conditioning phase 2. This effect might appear potentially consistent with the extensive animal literature on increased representation of CS^+ within auditory cortex (reviewed in refs. 4–6), although some of the single-cell findings from invasive animal recordings were at shorter latencies than the human N1m or P2m (e.g., refs. 1–3). The P1m differed here in showing higher amplitude for CS^- than CS^+ in phase 2 (Fig. 3). Although it might appear counterintuitive, there are some sparse previous reports (e.g., ref. 29) of enhanced responses for stimuli signaling safety (rather than shock) and here the CS^- was 100% informative of safety. Furthermore, we have since replicated the current phase-2 pattern for P1m in a further study.

However, for present purposes, the absolute sign of the change in P1m amplitude is less important than the existence of an amplitude difference indicating CS^+/CS^- differentiation for phase 2, even in the earliest component we studied. Some evidence of a brain-behavior dissociation was also noted for the P1m in the progressively reduced difference of responses to the CS^+ and CS^- during phase 2; as noted, this difference did not attain statistical significance across trials.

Whereas the P1m component readily distinguished CS^- from CS^+ in the initial phase of conditioning, it did not reverse its affiliation in phase 3 when the contingency changed. Instead the CS^+/CS^- differentiation disappeared for P1m in phase 3, as also for the conditioned pupil response (Fig. 1 *B* and *C*). This pattern contrasts with the P2m, which rapidly reversed its affiliation when the contingency reversed. The P2m (like the related P200 in past EEG studies) is well known to be a higher-order auditory component (e.g., ref. 30), that can be influenced by cognitive factors such as attention or expertise (e.g., ref. 31). The N1m component showed an intermediate outcome here, showing some degree of rapid plasticity when the contingency changed, in that the first bin of (new) CS^+ trials after reversal differed from the response to the same stimulus when serving as CS^- across phase 2. However, the N1m did not reverse its affiliation (i.e., the CS^+ and CS^- lines never cross over from phase 2 to phase 3 in Fig. 4*B*, unlike the P2m outcome). This N1m component (as for the potentially related N100 in past EEG studies) is generally considered as an intermediate-level auditory component, affected both by bottom-up factors and top-down influences such as attention (e.g., refs. 32, 33).

In sum, our key observation was that on the one hand, the auditory P1m, N1m, and P2m acted similarly in readily acquiring significant differentiation between CS^+/CS^- during the initial phase of conditioning (Fig. 3), whereas on the other hand, these components differed greatly in their sensitivity to the sudden contingency reversal, with the P2m alone showing sufficient flexibility to rapidly reverse its affiliation (Fig. 4).

P1m, N1m, and P2m are well-studied auditory-evoked field components. Their sources are thought to arise in medial aspects of primary auditory cortex in Heschl's gyrus for P1m, but predominantly in the planum temporale (secondary auditory cortex) for N1m. There is converging evidence for this from various source- localization techniques (34–37) as well as from invasive measures in animals (for review, ref. 14) and human patients (38). The P2m is likely to have several contributing sources, including activity in auditory association cortices, plus recurrent activation of primary and secondary auditory cortex (30). Given this strong existing evidence on the nature of sources for P1m, N1m, and P2m, and for their hierarchical nature (whereby each successive component reflects increasingly abstract levels of representation) (39), we did not revisit the source issue here. Instead, we show how these different hierarchical levels of auditory cortical processing are subject to different constraints for conditioning influences, especially in the face of contingency reversal.

Effects of aversive classical contingencies on auditory cortex, as studied here, are likely to involve contributions from brain areas beyond auditory cortex. The amygdala is known to be involved in aversive conditioning paradigms similar to that studied here (for review, ref. 40), as also evident from human neuroimaging studies using a variety of sensory stimuli (41, 42). The medial geniculate nucleus may work in concert with the amygdala for auditory fear conditioning (43).

Prefrontal cortex (PFC) is also known to be involved in conditioning paradigms, such as fear association due to shock. For instance, infralimbic prefrontal cortex (ventromedial PFC in primates) is important for extinction of conditioned responses (44; for review, refs. 45, 46), as evidently applied for the pupil measures in phase 3 here, and possibly for the P1m and N1m. Further frontal regions are important in reversal learning (9, 25, 47), so might relate to the influences we observed on the P2m here.

It may be noteworthy that amygdala circuits have typically been associated with relatively inflexible, cumulative "emotional" learning in several previous studies (9, 25). Frontal cir-

cuitry, by contrast, is thought to support more flexible learning on the basis of updated predictions, including those involved in reversals (9, 25, 47). We note also that the auditory P2m and the N1m (plus EEG analogs of these components) have been associated in the past with modulation by cognitive factors such as attention (32, 48), thought to arise due to influences from frontal cortex (32), whereas the P1m is typically found to be less influenced by putatively frontal influences such as attention (33).

This wider literature suggests one plausible framework for our findings, which leads also to new testable predictions. The rapid reversal in affiliation of the P2m when the contingency was reversed here may reflect cognitive top-down influences from frontal circuits upon auditory cortex, that can rapidly adapt to a change in contingency, affiliating with the tone that participants now expect to lead to shock (recall that our human participants were all aware of the contingency change, being informed before phase 3, just as they had been informed of the initial contingency in phase 2; *Materials and Methods*). By contrast, the impact of conditioning on the earlier, sensory P1m may reflect affective modulation by cumulative learning circuits, such as those within the amygdala, which are less able to reverse a well-established emotional association, thereby potentially explaining why the P1m did not reverse its affiliation here (but rather showed only extinction). Although our human participants could expect the previously unshocked tone to become paired with shock (consistent with the P2m outcome) when informed of this upcoming contingency reversal for phase 3, presumably they could not reverse the affective association of the previously shocked tone in phase 2 with an aversive outcome so readily (consistent with the P1m outcome). In future extensions of the present human MEG paradigm, it could be revealing to test whether the present modulations of auditory MEG components become pathologically absent in patients with intact auditory cortex but damage to PFC (which might knock out the rapid reversal of P2m affiliation) or to the amygdala (which might impair initial acquisition of CS^+/ CS^- differentiation for the P1m).

Relatively few previous studies have examined contingency reversal for classical conditioning in humans with neural measures. Two fMRI studies (9, 47) suggested roles for amygdala and PFC in Pavlovian fear-reversal paradigms (albeit for visual rather than auditory paradigms). Morris et al. (9) found that when the contingency reversed, the response in PFC switched rapidly but the amygdala response did not, in accord with our suggestions. If the P1m is indeed modulated by amygdala circuits (rather than by PFC circuits, as we suggest for the P2m instead), one needs to consider how this effect could arise for such a relatively early auditory response (latency of ~30 ms for the P1m). Several classic studies show that conditioned responses can arise at even faster latencies in the amygdala (e.g., ref. 49). Moreover, microstimulation of the amygdala can induce auditory plasticity (50). Finally, influences from the amygdala to auditory cortex are known to be cholinergically mediated (via nucleus basalis; e.g., ref. 43), raising the intriguing possibility of applying pharmacological manipulations (10, 51–53) to our human MEG paradigm in future work.

In conclusion, the present human MEG findings accord with a wide literature (1–3, 7, 52; reviewed in refs. 4–6) in showing plasticity of auditory cortex responses in animals, when sounds are paired with shock in a classical contingency. However, our findings go beyond previous observations in showing that different hierarchical levels of cortical auditory responses (P1m, N1m, and P2m) are subject to very different constraints in flexibility when faced with a sudden contingency reversal.

Materials and Methods

Participants. Nineteen adult volunteers (mean/SD age, 25.1/ 2.7 y, 10 females) were recruited via University College London's subject pool. All provided written consent was in accord with local ethical approval. None had a history of psychiatric or neurological illness on the basis of self-report. All were right handed.

Stimuli and Task. Auditory stimuli were presented binaurally, via piezo-driven loudspeakers connected via air tubes to MEG-compatible in-ear headphones

(Etymotics), with loudness adjusted to 70 dB sound pressure level. To encourage them to listen and remain alert, participants performed an incidental oddball-detection task, pressing a button with the right hand for rare oddball sounds that were longer (400 ms) than standard (200 ms) sounds, while fixating a central cross. Rare longer oddballs (10% of all stimuli) were embedded in random sequences of pure tones of two frequencies (1.5 kHz and 4 kHz, 10 ms linear rise and decay for all tones), with one tone presented at a time. Stimuli were presented in blocks of 120 (60 at each pitch), lasting roughly 2 min, with stimulus onset asynchronies of 750–1,150 ms. There were three phases: baseline (4 blocks), initial conditioning (14 blocks), and contingency reversal (14 blocks). The baseline phase 1 (without conditioning) comprised 480 stimuli in total. Subsequent phase 2 comprised initial conditioning, with one of the frequencies (CS^+) but not the other (CS^-) paired with shock unconditioned stimulus (US) 50% of the time. The tone frequency serving as CS^+ was counterbalanced across participants. When paired with the US, CS^+ was followed by a train of three electrical stimuli on the left forearm (at 100, 175, and 250 ms posttone onset). Before the experiment, participants rated electrical forearm stimulation of increasing intensity on an aversiveness scale, between 1 and 10. The intensity associated with a rating of 7 was chosen for use in the experiment (leading to a mean ± SD value of 32.6 ± 6.2 mA), with each shock lasting 1 ms. In phase 2, participants were exposed to 840 stimuli of each pitch, with half the CS^+ stimuli being reinforced with the US shock. Phase 2 allowed us to test whether differences in evoked auditory fields (for P1m, N1m, and P2m; ref. 35) would emerge between CS^+ and CS^- for initial conditioning. Participants were verbally informed of the nature of the shock contingency before phase 2.

In phase 3, the contingencies were abruptly reversed, i.e., the previous CS^+ tone now became the CS^- tone and vice versa. Participants were verbally informed that this reversal would now take place (which can be readily done in human participants, less readily in other species without overtraining and secondary associations) just before the start of phase 3. This procedure ensured that they could now expect the opposite contingency, thereby allowing any possible top-down modulation (*Discussion*). As in phase 2, participants were exposed to 840 stimuli of each tone frequency, with half the new CS^+ stimuli (former CS^-) now being reinforced with the US shock.

In all three phases, participants were given feedback on the oddball duration detection task in percent correct (which averaged 87 ± 4.7% over the entire experiment) at the end of each block. Duration oddballs were equally likely to occur for tones at either frequency (10% of all trials), regardless of which might be associated with shock. Oddball trials were subsequently discarded from the MEG data, so our analyses focused on auditory responses to the standard tones not requiring an overt manual response.

For MEG recordings, subjects were first familiarized with the oddball-duration task, which required them to press a button with their right hand whenever a longer tone appeared, and given the opportunity to practice. As outlined above, the recording session comprised 32 blocks in total, resulting in ~1 h of recording time.

MEG Recording Parameters. Neuromagnetic activity was recorded using a whole-head 275-channel axial gradiometer MEG system (CTF Systems). In addition, the electrocardiogram and vertical and horizontal electrooculograms (EOGs) were recorded through bipolar montages. Head position relative to MEG sensors was measured at the beginning and end of the recording session using a standard localization coil setup. One coil was placed on the nasion, the other two coils were mounted onto the earpieces that held the tubes for pneumatic auditory stimulation, such that the tubes ran through the middle of the magnetic coils. MEG data were low-pass filtered at 150 Hz and sampled continuously at a rate of 600 Hz.

Data Analysis. Data were analyzed using the Fieldtrip software package alongside SPM8 for EEG/MEG. Data were checked for artifacts using a semi-automatic routine that detects and rejects eye blinks, muscle artifacts, and occasional jumps in the MEG signal due to the super-conducting quantum interference device (SQUID) electronics, as reported previously (54). Rejection thresholds were set on an individual participant level, on the basis of the entire dataset before splitting it into conditions. Thus, the artifact rejection routines were fully independent of the conditions and contrasts reported here, hence unbiased.

The artifact-free data were interpolated to a common sensor-array template using a minimum-norm projection method (54). Artifact-corrected raw data were low-pass filtered (cutoff frequency set to 30 Hz), averaged, baseline corrected (baseline from 100 ms preceding tone onset), and interpolated to the common sensor array. The planar field gradient simplifies interpretation of the sensor-level data, because the maximal signal is more typically located above the source (54). Accordingly, planar gradients of the MEG field distribution were calculated using a nearest neighbor, as used

previously (54). The obtained realigned planar gradients were then grand averaged to obtain average topographies. For the P1m component, given its early onset, we analyzed CS⁺ presentations with and without successive US presentation (which could start only 100 ms after the tone) together. For later components (N1m and P2m), we analyzed only that half of the CS⁺ trials not followed by shock, so that occurrence of the latter could not contaminate our auditory MEG measures.

Eye Tracking. We used an infrared eye-tracker (Eyelink 1000) to monitor subjects' pupil diameter throughout the experiment, along with eye position, sampled at 600 Hz. The pupil diameter time courses were then z scored and subjected to similar artifact rejection routines as described for MEG analysis. Pupil data were then analyzed in a time-locked manner, using the fieldtrip software package as well as custom Matlab routines for detection and rejection of any periods during which saccades occurred. The latter segments were not included in any further analyses.

1. Edeline JM, Weinberger NM (1993) Receptive field plasticity in the auditory cortex during frequency discrimination training: Selective retuning independent of task difficulty. *Behav Neurosci* 107:82–103.
2. Bakin JS, Weinberger NM (1990) Classical conditioning induces CS-specific receptive field plasticity in the auditory cortex of the guinea pig. *Brain Res* 536:271–286.
3. Diamond DM, Weinberger NM (1986) Classical conditioning rapidly induces specific changes in frequency receptive fields of single neurons in secondary and ventral ectosylvian auditory cortical fields. *Brain Res* 372:357–360.
4. Weinberger NM (2004) Specific long-term memory traces in primary auditory cortex. *Nat Rev Neurosci* 5:279–290.
5. Irvine DRF (2007) Auditory cortical plasticity: Does it provide evidence for cognitive processing in the auditory cortex? *Hear Res* 229:158–170.
6. Weinberger NM (2007) Associative representational plasticity in the auditory cortex: A synthesis of two disciplines. *Learn Mem* 14:1–16.
7. Polley DB, Steinberg EE, Merzenich MM (2006) Perceptual learning directs auditory cortical map reorganization through top-down influences. *J Neurosci* 26:4970–4982.
8. Molchan SE, Sunderland T, McIntosh AR, Herscovitch P, Schreurs BG (1994) A functional anatomical study of associative learning in humans. *Proc Natl Acad Sci USA* 91:8122–8126.
9. Morris JS, Friston KJ, Dolan RJ (1998) Experience-dependent modulation of tonotopic neural responses in human auditory cortex. *Proc Biol Sci* 265:649–657.
10. Thiel CM, Friston KJ, Dolan RJ (2002) Cholinergic modulation of experience-dependent plasticity in human auditory cortex. *Neuron* 35:567–574.
11. Moses SN, Bardouille T, Brown TM, Ross B, McIntosh AR (2010) Learning related activation of somatosensory cortex by an auditory stimulus recorded with magnetoencephalography. *Neuroimage* 53:275–282.
12. Moses SN, Martin T, Houck JM, Ilmoniemi RJ, Tesche CD (2005) The C50m response: Conditioned magnetocerebral activity recorded from the human brain. *Neuroimage* 27:778–788.
13. Jacobson GP (1994) Magnetoencephalographic studies of auditory system function. *J Clin Neurophysiol* 11:343–364.
14. Näätänen R, Picton T (1987) The N1 wave of the human electric and magnetic response to sound: A review and an analysis of the component structure. *Psychophysiology* 24:375–425.
15. Begleiter H, Platz A (1969) Evoked potentials: Modifications by classical conditioning. *Science* 166:769–771.
16. Miltner WH, Braun C, Arnold M, Witte H, Taub E (1999) Coherence of gamma-band EEG activity as a basis for associative learning. *Nature* 397:434–436.
17. Skrandies W, Jedynak A (2000) Associative learning in humans—conditioning of sensory-evoked brain activity. *Behav Brain Res* 107:1–8.
18. Oleson TD, Westenberg IS, Weinberger NM (1972) Characteristics of the pupillary dilation response during Pavlovian conditioning in paralyzed cats. *Behav Biol* 7:829–840.
19. Oleson TD, Ashe JH, Weinberger NM (1975) Modification of auditory and somatosensory system activity during pupillary conditioning in the paralyzed cat. *J Neurophysiol* 38:1114–1139.
20. Ryugo DK, Weinberger NM (1978) Differential plasticity of morphologically distinct neuron populations in the medial geniculate body of the cat during classical conditioning. *Behav Biol* 22:275–301.
21. Ashe JH, Cooper CL, Weinberger NM (1978) Role of the parasympathetic pupillomotor system in classically conditioned pupillary dilation of the cat. *Behav Biol* 23:1–13.
22. Cassady JM, Farley GR, Weinberger NM, Kitzes LM (1982) Pupillary activity measured by reflected infra-red light. *Physiol Behav* 28:851–854.
23. Hermans D, Craske MG, Mineka S, Lovibond PF (2006) Extinction in human fear conditioning. *Biol Psychiatry* 60:361–368.
24. Quirk GJ, et al. (2010) Erasing fear memories with extinction training. *J Neurosci* 30:14993–14997.
25. Schiller D, Delgado MR (2010) Overlapping neural systems mediating extinction, reversal and regulation of fear. *Trends Cogn Sci* 14:268–276.
26. Sehlmeyer C, et al. (2009) Human fear conditioning and extinction in neuroimaging: A systematic review. *PLoS ONE* 4:e5865.
27. Liu J, Harris A, Kanwisher N (2002) Stages of processing in face perception: An MEG study. *Nat Neurosci* 5:910–916.
28. Kriegeskorte N, Simmons WK, Bellgowan PSF, Baker CI (2009) Circular analysis in systems neuroscience: The dangers of double dipping. *Nat Neurosci* 12:535–540.
29. Pizzagalli DA, Greischar LL, Davidson RJ (2003) Spatio-temporal dynamics of brain mechanisms in aversive classical conditioning: High-density event-related potential and brain electrical tomography analyses. *Neuropsychologia* 41:184–194.
30. Tarkka IM, Stokić DS, Basile LF, Papanicolaou AC (1995) Electric source localization of the auditory P300 agrees with magnetic source localization. *Electroencephalogr Clin Neurophysiol* 96:538–545.
31. Kuriki S, Kanda S, Hirata Y (2006) Effects of musical experience on different components of MEG responses elicited by sequential piano-tones and chords. *J Neurosci* 26:4046–4053.
32. Woldorff MG, et al. (1993) Modulation of early sensory processing in human auditory cortex during auditory selective attention. *Proc Natl Acad Sci USA* 90:8722–8726.
33. Okamoto H, Stracke H, Bermudez P, Pantev C (2010) Sound processing hierarchy within human auditory cortex. *J Cogn Neurosci* 23:1855–1863.
34. Kanno A, Nakasato N, Murayama N, Yoshimoto T (2000) Middle and long latency peak sources in auditory evoked magnetic fields for tone bursts in humans. *Neurosci Lett* 293:187–190.
35. Pantev C, Hoke M, Lütkenhöner B, Lehnertz K (1991) Neuromagnetic evidence of functional organization of the auditory cortex in humans. *Acta Otolaryngol Suppl* 491:106–114, discussion 115.
36. Reite M, et al. (1994) Auditory M100 component 1: Relationship to Heschl's gyri. *Brain Res Cogn Brain Res* 2:13–20.
37. Yamamoto T, Williamson SJ, Kaufman L, Nicholson C, Llinás R (1988) Magnetic localization of neuronal activity in the human brain. *Proc Natl Acad Sci USA* 85:8732–8736.
38. Godey B, Schwartz D, de Graaf JB, Chauvel P, Liégeois-Chauvel C (2001) Neuromagnetic source localization of auditory evoked fields and intracerebral evoked potentials: A comparison of data in the same patients. *Clin Neurophysiol* 112:1850–1859.
39. Lütkenhöner B, Steinsträter O (1998) High-precision neuromagnetic study of the functional organization of the human auditory cortex. *Audiol Neurootol* 3:191–213.
40. Pape H-C, Pare D (2010) Plastic synaptic networks of the amygdala for the acquisition, expression, and extinction of conditioned fear. *Physiol Rev* 90:419–463.
41. Gottfried JA, Dolan RJ (2004) Human orbitofrontal cortex mediates extinction learning while accessing conditioned representations of value. *Nat Neurosci* 7:1144–1152.
42. Phelps EA, Delgado MR, Nearing KI, LeDoux JE (2004) Extinction learning in humans: Role of the amygdala and vmPFC. *Neuron* 43:897–905.
43. Weinberger NM (2010) The medial geniculate, not the amygdala, as the root of auditory fear conditioning. *Hear Res* 274:61–74.
44. Quirk GJ, Russo GK, Barron JL, Lebron K (2000) The role of ventromedial prefrontal cortex in the recovery of extinguished fear. *J Neurosci* 20:6225–6231.
45. Quirk GJ, Mueller D (2008) Neural mechanisms of extinction learning and retrieval. *Neuropsychopharmacology* 33:56–72.
46. Sotres-Bayon F, Quirk GJ (2010) Prefrontal control of fear: More than just extinction. *Curr Opin Neurobiol* 20:231–235.
47. Schiller D, Levy I, Niv Y, LeDoux JE, Phelps EA (2008) From fear to safety and back: Reversal of fear in the human brain. *J Neurosci* 28:11517–11525.
48. Hillyard SA, Hink RF, Schwent VL, Picton TW (1973) Electrical signs of selective attention in the human brain. *Science* 182:177–180.
49. Quirk GJ, Repa C, LeDoux JE (1995) Fear conditioning enhances short-latency auditory responses of lateral amygdala neurons: Parallel recordings in the freely behaving rat. *Neuron* 15:1029–1039.
50. Chavez CM, McGaugh JL, Weinberger NM (2009) The basolateral amygdala modulates specific sensory memory representations in the cerebral cortex. *Neurobiol Learn Mem* 91:382–392.
51. Bakin JS, Weinberger NM (1996) Induction of a physiological memory in the cerebral cortex by stimulation of the nucleus basalis. *Proc Natl Acad Sci USA* 93:11219–11224.
52. Butt AE, et al. (2009) Association learning-dependent increases in acetylcholine release in the rat auditory cortex during auditory classical conditioning. *Neurobiol Learn Mem* 92:400–409.
53. Miasnikov AA, Chen JC, Weinberger NM (2006) Rapid induction of specific associative behavioral memory by stimulation of the nucleus basalis in the rat. *Neurobiol Learn Mem* 86:47–65.
54. Bauer M, Oostenveld R, Peeters M, Fries P (2006) Tactile spatial attention enhances gamma-band activity in somatosensory cortex and reduces low-frequency activity in parieto-occipital areas. *J Neurosci* 26:490–501.